MODELLING AND QUANTIFYING MODE I INTERLAMINAR FRACTURE IN PARTICLE-TOUGHENED CFRPS

G. Borstnar[1], M.N. Mavrogordato[1], Q.D. Yang[2], I. Sinclair[1] and S.M. Spearing[1]

[1]Faculty of Engineering and the Enviroment, Univertity of Southampton, Southampton, United Kingdom
Email: G.Borstnar@soton.ac.uk, Web Page: http://www.southampton.ac.uk/
[2]Department of Mechanical and Aerospace Engineering, University of Miami, Coral Gables, Florida, United States of America Country
Email: qdyang@miami.edu, Web Page: http://welcome.miami.edu/

Abstract
Four-dimensional time-resolved Synchrotron Radiation Computed Tomography (SRCT) has been used to capture Mode I delamination propagation in particle-toughened Carbon Fibre Reinforced Polymers (CFRPs). Digital Volume Correlation (DVC) was used in order to measure ply opening displacements at the crack tip, permitting the interlayer strain ahead of the crack tip to be quantified. Estimates at which toughening particles de-bonded and/or fractured were made, giving insight into the effects of particle type and particle size on the fracture mico-mechanisms. The experiments are complemented by a 2D plane-strain finite element (FE) model, which investigated the effects of particle strength and toughness on the ply opening displacement and crack path by modelling the particles as 1D cohesive segments. Previous work has shown that Mode I crack propagation in particle-toughened interlayers involves a process zone rather than a distinct crack tip. Therefore, Augmented Finite Element Method (A-FEM) elements were used in the simulation, since the elements can account for both bifurcating and merging cracks within a single element. The nodal displacements in the simulation were compared to the DVC results, illustrating a potential path through which more complex FE simulations may be validated against experimental results in the future.

1. Introduction

Low velocity impacts have been shown to significantly reduce the mechanical properties of Carbon Fibre Reinforced Polymers (CFRPs), which are evermore present in primary aerospace structures. Secondary-phase particles dispersed within interlaminar regions have been shown to suppress the spread of delaminations via toughening of the interlayer [1]–[3]. Crack initiation and propagation in these interlayers is not well understood, but through the use of Synchrotron Radiation Computed Tomography (SRCT), *in situ* non-destructive imaging of the sequence of crack tip processes is possible with time-resolved experiments. Additionally, the 3D datasets between crack load steps can be used to track internal displacements via the Digital Volume Correlation (DVC) technique [4]. DVC is essentially a 3D version of Digital Image Correlation (DIC), and has been shown to track displacements successfully perpendicular to the fibre direction [5]. Currently, models accounting for the effects of particles, within the constraints of a laminate, on the crack path and fracture toughness have not yet been developed. Understanding and modelling the crack path is important because it has been shown experimentally that the crack growth resistance can decrease when the crack path deviates from the toughened interlayer to the ply interface [6], [7].

In this work, crack propagation through particle-toughened interlayers was captured in four different material systems. DVC was performed on the data, allowing the interlayer strains to be quantified, along with a measure of crack flank displacement. Two distinct particle types within each material system had a significant effect on the formation of bridging ligaments and their composition. An assessment of the strain at which micro-mechanical events occur was made; including, the internal fracture and de-bonding of particles. The work introduces a 2D plane-strain model, in which particles were modelled using 1D cohesive segments within an interlayer. The elemental displacements of the plies for a 'propagating' crack were compared for different particle properties/configurations and to the DVC measurements. This work provides insight as to; (a) what information can be obtained through DVC regarding the micromechanical processes and whether this can inform models, and (b) which material parameters influence the simulated crack path and the ply opening displacement.

2. Methods

### 2.1. Materials and specimen geometries

Proprietary and developmental CFRPs were manufactured by the Cytec Solvay Group and cured according to a standard aerospace cycle. 16-ply uni-directional panels were laid up with a 40 μm thick Polytetraflouroethylene (PTFE) insert placed at mid-plane along one edge of the plate. The materials studied had secondary phase particles dispersed within the interlayer at a 13 % volume fraction, with the bulk resin and intermediate modulus carbon fibre remaining consistent between the material systems. Two different particle types were used; Mat. A – featured particles that fracture internally, and Mat. B – featured particles that de-bond from the surrounding resin. Three different particle size distributions were considered for the Mat. B particles, small (S) – denoting particles of about 10 μm in diameter, large (L) – denoting particles of about 30 μm in diameter, and a hybrid of both the small and the large particles (S+L). The normalized Mode I initiation fracture toughness (G_{IC}) for Mat. A, Mat. B(S), Mat. B(L) and Mat. B(S+L) were 1.0, 0.8, 0.58 and 0.55 respectively. Specimens were cut from the manufactured panels into 2.5 mm (wide) x 3.0 mm (thick) x 120 mm (long) geometries, with the small cross-section chosen in order to maximize the transmission of low energy photons.

2.2 SRCT experiments and DVC analysis

A purpose built *in situ* loading device was used to drive a wedge into the mid-plane of the CFRP samples at the insert in order to generate the Mode I opening loads. The crack was extended about 5 mm from the end of the insert, following which the specimen was scanned. Subsequently, the wedge was driven further into the sample in a displacement-controlled manner, extending the crack further. The same regions in the specimen were then scanned again, permitting the crack extension to be captured in 3D. SRCT experiments were conducted at the Swiss Light Source on the TOMCAT beamline at the Paul Scherrer Insitut, Villigen, Switzerland. A voxel resolution of 0.325 μm was used, with a detector size of 2560 x 2160 pixels. 1501 projections were taken at an exposure of 150 ms for the 180-degree rotation. A beam energy of 15 kV was used, while a propagation distance of 23 mm emphasized the edges between materials of similar attenuation via phase-enhance contrast [8]. The CT data was reconstructed using the in-house GRIDREC method [9]. The datasets were then reduced to 8-bit format for DVC processing in DaVis 8.1.3 software (LaVision, Goettingen, Germany, 2012) via a proprietary Fast Fourier Transform (FFT) approach. A noise study was used to evaluate the strain resolution of the measurements and is outlined in [5].

G. Borstnar, M.N. Mavrogordato, Q.D. Yang, I. Sinclair and S.M. Spearing

2.3 A-FEM simulation

The 2D plane-strain model was implemented in Abaqus FEA version 6.12 (Dassault Systemes, Velizy-Villacoublay, France) with user subroutines. Standard CPS4 elements defined the neighbouring ply properties, and the 'crackable' resin, particle and ply interfaces were defined by A-FEM elements. 2D A-FEM elements developed by Liu et al. [10] were used, since these have been shown to account for arbitrary intra-element cracks and their interactions. The A-FEM elements can crack without *a priori* knowledge and the separation of the discontinuity is defined by a bilinear cohesive law. The resin, plies and ply-interface properties are kept consistent throughout all of the presented simulations. Only the properties of the 1D 'particles' were altered between the presented simulation. In this paper, particle cohesive strengths of 0 MPa, 1 MPa and 30 MPa are considered, whilst maintaining a resin strength of 50 MPa. The toughness of the resin was 0.0125 J/mm^2, while the 'particles' had a toughness of 0.02 J/mm^2 in order to simulate particle-bridging effects. Figure 1 illustrates the 2D model, where an initial starter crack is used to bring the crack towards the region of interest (ROI). Within this region, the 1D segments define the particles and the ply interfaces, and the 'particle' fraction was maintained at 50 % for the presented results. The thickness of the interlayer is consistent with the ~30 μm interlayers seen in the CT data, and the displacement-controlled loading conditions were applied 0.33 mm (< x10 of an interlayer thickness) away from the start of the ROI.
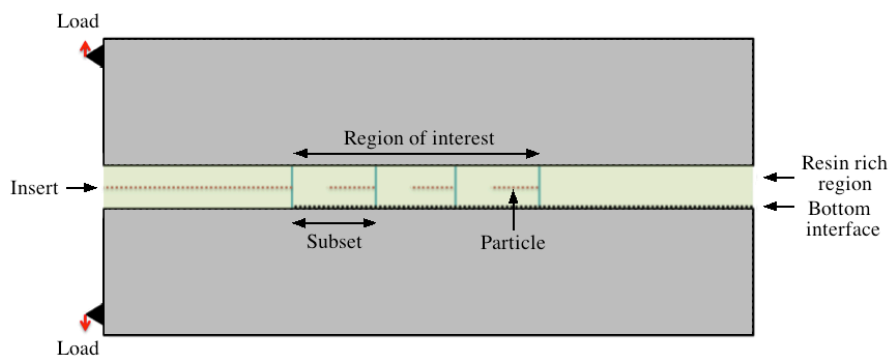

**Figure 1.** Schematic of the Mode I interlayer model

3. Results

3.1 Interlayer opening strain measurements

Figure 2 shows a 3D view of the tensile opening strains (perpendicular to the ply orientation) captured via DVC analysis. The strains presented range between 0.1-3.0 %, since at above 3 % strain, there is too many new crack surfaces appearing in the subvolumes between the load steps. This reduces the correlation achieved between the subvolumes, and hence increases the uncertainty in the exact placement of the subvolume in following the loadstep. This is important because the strains in the presented work are calculated as the relative change in distance between the centroids of the neighbouring subvolumes. The noise study (detailed in [5]) determined that a conservative estimate of the strain resolution is 0.1 %, so any strain that is recorded to be higher than this value is a result of material deformation rather than due to noise in the data. Interestingly, Figure 2 shows that strains greater than 0.1 % were measured in the neighbouring ply interlayers both above and below the crack tip, which in Mat. A was sufficient to fracture a number of particles. Additionally, in the mid-plane, there is a clear decrease in opening strain as the distance from the crack tip increased, allowing the opening strain profile to be plotted with respect to the position along the crack.

G. Borstnar, M.N. Mavrogordato, Q.D. Yang, I. Sinclair and S.M. Spearing
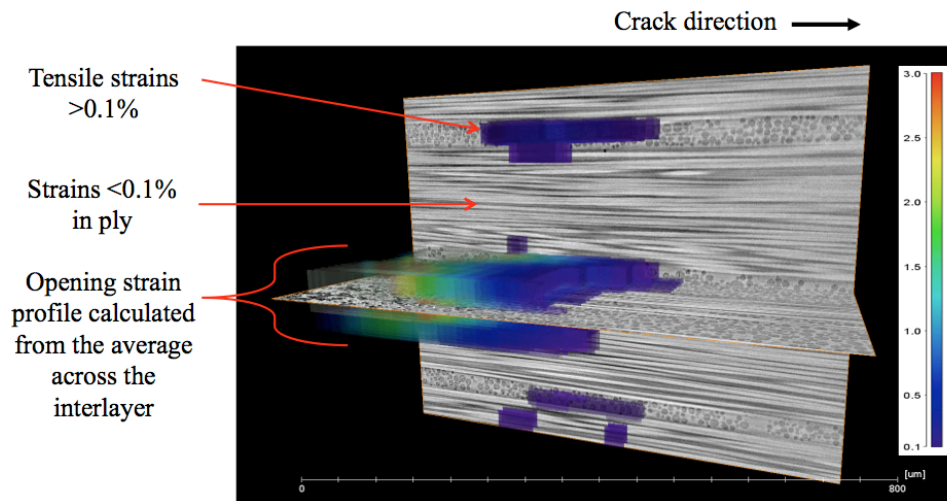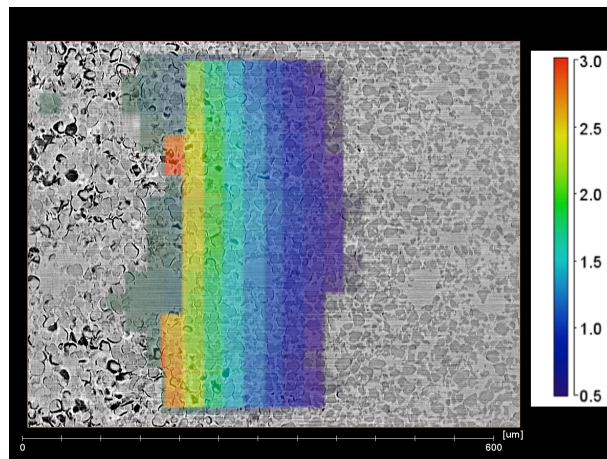
Crack direction ⟶

Figure 2. 3D illustration of the measured strains at and ahead of a Mode I crack tip in Mat. A

Figure 3 emphasizes that DVC permits the strains to be evaluated within the constraints of a laminate and in the through-the-width direction, which (to the best of the authors' knowledge) cannot be measured directly in any other way. The top-down view onto the micro-structure permits the local tensile interlayer strains at which the particles fracture or de-bond to be estimated. Figure 3(a) shows the strains ahead of the crack tip in Mat. A. Crack propagation in this material system initiates from the particles fracturing internally, to crack coalescence, and the formation of particle-bridging ligaments in the crack wake (as previously determined in [5]). The DVC data suggests that the internal particle fracture occurs at about 0.5 % opening strain, with little evidence of particle/resin de-bonding until above 2 % opening strain. Even so, the particle adhesion to the matrix appears to be strong, enabling the themorplastic ligaments to yield and provide energy-dissipating/toughness-enhancing traction forces across the crack flanks. Figure 3(a) and (b) show the opening strains in the Mat. B (S) and Mat. B(L) systems. The data shows that the smaller particles de-bond at significantly higher strains that the large-particle system, where there is clear de-bonding occurring at about 0.5 % strain. The smaller particles appear to de-bond at around 1 %, and do not de-bond to the same extent as the larger particles, which appear to be almost completely de-bonded. Dissimilar to Mat. A, the Mat. B particle type features damage propagation through initial particle/resin de-bonding, following which resin ligaments, formed from the epoxy between the particles, bridge the crack flanks.

G. Borstnar, M.N. Mavrogordato, Q.D. Yang, I. Sinclair and S.M. Spearing
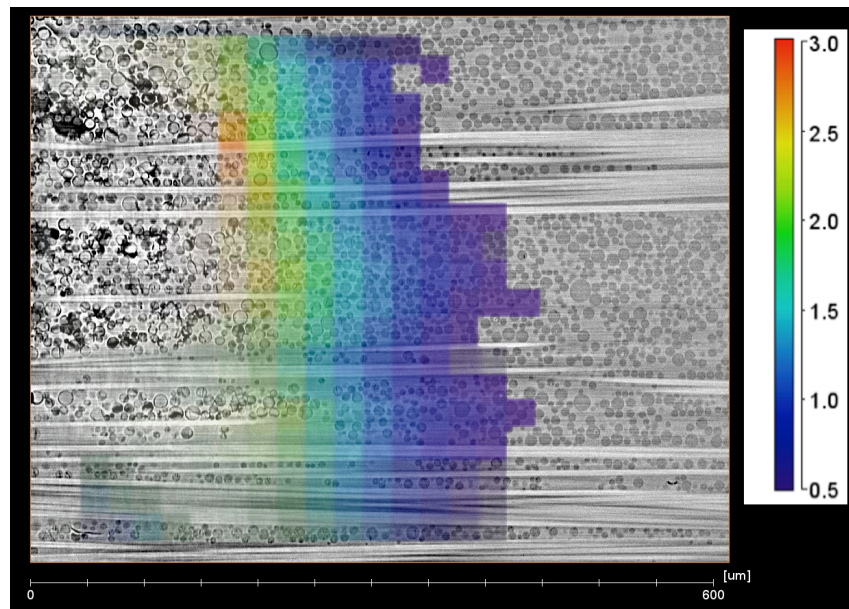
(a)
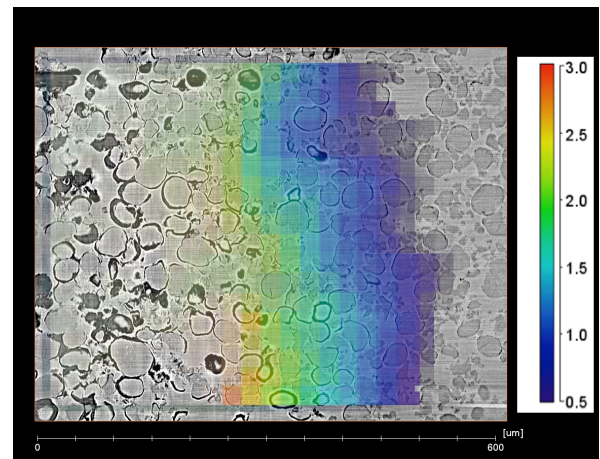
(b)   (c)

Figure 3. Top-down view of the material micro-structure with tensile opening strain (%) overlaid for;
(a) Mat. A, (b) Mat. B(S), and (c) Mat. B(L), with the crack direction from left-to-right

G. Borstnar, M.N. Mavrogordato, Q.D. Yang, I. Sinclair and S.M. Spearing

3.2 Comparison between simulation and experiments

Figure 4(a) shows a plot of the nodal displacements of the top-ply interface of the interlayer model. The data shows a 'propagating' crack state, in which the simulation was stopped when a specified resin A-FEM element cracked (at about 21% into the ROI). The particles in this simulation were about twice the toughness of the surrounding resin, but had a much lower initiation stress than that of the resin (50 MPa), in order to simulate de-bonding or a separation via internal cracking. The A-FEM simulation successfully accounted for the merging of the cracks between the resin and particle elements, allowing the effects of particle strength to be explored. Figure 4(a) shows the relevant positions of the beginning of the ROI (end of the insert) and the position of the continuous crack tip. As the strength of the particle was increased, the gradient of the nodal displacements increased, which is consistent with a tougher or stiffer interlayer behaviour under displacement-controlled loading conditions. In the presented cases, the crack path was maintained within the interlayer, but if the particle strength was increased above 30 MPa, the crack path transitioned to the competing crack path along the ply interface. Figure 4(b) shows the average tensile opening of the materials considered in this work, with an indication of the relevant micro-mechanisms and associated level of strains annotated on the y-axis. The results indicate that the strain opening profile may be comparable to future simulation results, but the correlation between the material G_{IC} and the strain profiles presented is unclear, since the gradient of the Mat. B(S+L) is expected to be the shallowest.
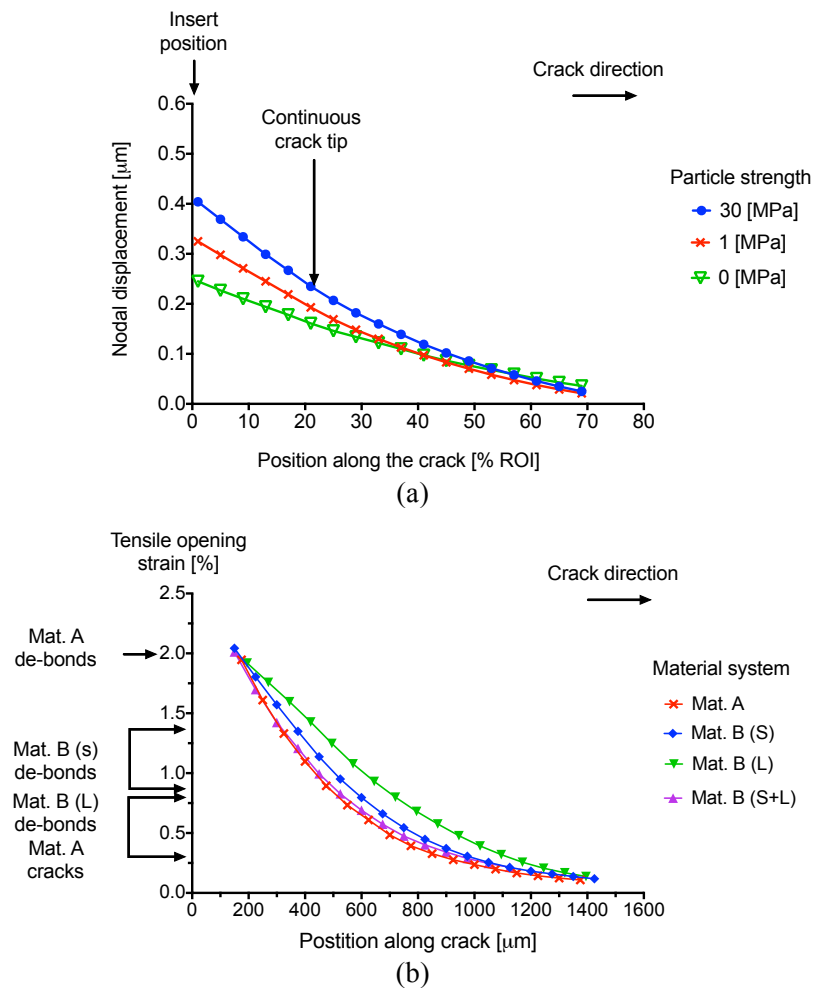
Figure 4. Plots comparing the relative ply opening displacement and tensile opening strains against an arbitrary crack position with data obtained from; (a) the A-FEM simulation, and (b) the DVC analysis

G. Borstnar, M.N. Mavrogordato, Q.D. Yang, I. Sinclair and S.M. Spearing

4. Conclusions

Overall, the presented work has shown that DVC is a powerful technique that can provide estimates of the local strains at which micro-mechanical events occur. It is thought that such estimates may be useful to determining materials properties, such as particle-interface strengths, which are difficult to measure experimentally. The strain data presented suggests that the larger Mat. B particles tend to de-bond at lower tensile stresses, and that the Mat. A particles have a better adhesion to the resin due to de-bonding events occurring at higher local strains. The work has also identified that the strains in the neighbouring interlayers, in some materials, are enough to cause additional damage that may inadvertently contribute to the measured G_{IC}. The FE simulation showed that the particle strength can be used to control the crack path, while keeping other variables constant. Provided that the crack path remained interlaminar, the nodal/crack flank displacement gradient decreased with a decreasing particle strength, consistent with a less tough or a less stiff interlayer. It is expected that such data rich mechanics experiments, utilizing CT and associated quantification techniques, can be used in the development, calibration and/or validation of future micro-mechanical models.

References

[1]   M. Yasaee, I. P. Bond, R. S. Trask, and E. S. Greenhalgh, "Mode II interfacial toughening through discontinuous interleaves for damage suppression and control," *Compos. Part A Appl. Sci. Manuf.*, vol. 43, no. 1, pp. 121–128, Jan. 2012.

[2]   M. Yasaee, I. P. Bond, R. S. Trask, and E. S. Greenhalgh, "Mode I interfacial toughening through discontinuous interleaves for damage suppression and control," *Compos. Part A Appl. Sci. Manuf.*, vol. 43, no. 1, pp. 198–207, Jan. 2012.

[3]   D. J. Bull, A. E. Scott, S. M. Spearing, and I. Sinclair, "The influence of toughening-particles in CFRPs on low velocity impact damage resistance performance," *Compos. Part A Appl. Sci. Manuf.*, vol. 58, pp. 47–55, Mar. 2014.

[4]   T. S. Smith, B. K. Bay, and M. M. Rashid, "Digital Volume Correlation Including Rotational Degrees of Freedom during Minimization," *Exp. Mech.*, vol. 42, no. 3, pp. 272–278, 2002.

[5]   G. Borstnar, F. Gillard, M. N. Mavrogordato, I. Sinclair, and S. M. Spearing, "Three-dimensional deformation mapping of Mode I interlaminar crack extension in particle-toughened interlayers," *Acta Mater.*, vol. 103, no. C, pp. 63–70, 2016.

[6]   M. Hojo, S. Matsuda, M. Tanaka, S. Ochiai, and A. Murakami, "Mode I delamination fatigue properties of interlayer-toughened CF/epoxy laminates," *Compos. Sci. Technol.*, vol. 66, no. 5, pp. 665–675, May 2006.

[7]   N. Sela and O. Ishai, "Interlaminar fracture toughness and toughening of laminated composite materials: A review," *Composites*, vol. 20, no. 5, pp. 423–35, 1989.

[8]   P. Cloetens, M. Pateyron-Salomé, J. Y. Buffière, G. Peix, J. Baruchel, F. Peyrin, and M. Schlenker, "Observation of microstructure and damage in materials by phase sensitive radiography and tomography," *J. Appl. Phys.*, vol. 81, no. 9, p. 5878, 1997.

[9]   F. Marone and M. Stampanoni, "GRIDREC software," *J. Synchrotron Rad.*, vol. 19, pp. 1029–1037, 2012.

[10] W. Liu, Q. D. Yang, S. Mohammadizadeh, and X. Y. Su, "An efficient augmented finite element method for arbitrary cracking and crack interaction in solids," *Int. J. Numer. Methods Eng.*, vol. 99, no. May, pp. 438–468, 2014.